



# Multilayer Oxygen-Scavenging Biodegradable Polylactic Acid Films Reinforced with Microcrystalline Cellulose and Butylated Hydroxytoluene: Experimental Study of Structure-Property-Function Relationships Completed with Bibliometric Analysis toward Sustainable Development Goals (SDGs)

Andi Dirpan<sup>1\*</sup>, Mulyati M. Tahir<sup>1</sup>, Serli Hatul Hidayat<sup>1</sup>, Abel Yandi Novrain<sup>1</sup>, Soumya Majumder<sup>1,2</sup>,  
Eng Keng Seow<sup>3</sup>

<sup>1</sup>Hasanuddin University, Makassar, Indonesia

<sup>2</sup>Darjeeling Tea Research and Development Centre, Darjeeling, India.

<sup>3</sup>Universiti Teknologi MARA, Shah Alam, Selangor, Malaysia

\*Correspondence: E-mail: [dirpan@unhas.ac.id](mailto:dirpan@unhas.ac.id)

## ABSTRACT

This study presents an experimental investigation of multilayer oxygen-scavenging biodegradable polylactic acid films reinforced with microcrystalline cellulose (MCC) derived from nata de coco and butylated hydroxytoluene (BHT), completed with a bibliometric analysis. Structure-property-function relationships were evaluated through morphology, mechanical performance, oxygen permeability, and biodegradability analyses. fMCC enhances matrix densification and mechanical strength while reducing oxygen permeability, although flexibility decreases. The incorporation of BHT further improves oxygen-scavenging performance. These findings support the development of advanced biodegradable packaging aligned with sustainable development goals (SDGs).

## ARTICLE INFO

### Article History:

Submitted/Received 12 Dec 2025

First Revised 13 Feb 2026

Accepted 01 Apr 2026

First Available online 05 May 2026

Publication Date 01 Mar 2027

### Keyword:

Biodegradable;

Butylated hydroxytoluene;

Microcrystalline cellulose;

Polylactic acid;

Sustainable.

## 1. INTRODUCTION

The demand for safe, environmentally friendly food packaging that can maintain product quality continues to increase. This has driven the development of biodegradable packaging technology as an alternative to conventional plastic. Synthetic plastics such as LDPE and HDPE have excellent oxygen barrier properties, but they are not easily degradable, leading to long-term environmental issues [1]. On the other hand, biopolymers such as polylactic acid (PLA) and starch have advantages in terms of biodegradability. However, the integration of plastic with microcrystalline cellulose (MCC) as a reinforcing material and butylated hydroxytoluene (BHT) as an oxygen scavenger has not been widely developed. Therefore, the development of bioplastic materials with improved barrier and mechanical properties is crucial, especially for applications in food products that are susceptible to oxidative damage.

One emerging approach is the use of fillers such as MCC as a reinforcing filler in biopolymer matrices. Various studies indicate that MCC can increase the density of the matrix structure through the formation of a strong hydrogen bonding network, thereby enhancing mechanical strength and reducing gas permeability [2, 3]. In addition, the integration of active compounds such as BHT as an oxygen scavenger in active packaging systems is an effective strategy to inhibit oxidation reactions by donating hydrogen atoms to stabilize free radicals [4]. The combination of MCC as a structural enhancer and BHT as an active agent opens up opportunities in the development of biopolymer-based active packaging with improved performance.

Various previous studies have shown that the addition of MCC to bioplastics can improve mechanical and barrier properties, and the use of multilayer systems can enhance the efficiency of oxygen diffusion inhibition [5, 6]. In addition, the development of antioxidant-based active packaging has also been proven to slow down oxidative degradation in food products, including oxygen-absorbing agents [7-9]. However, most studies still focus on improving only one aspect, either mechanical properties or functional activity, and there has been little research that simultaneously integrates MCC from natural sources, such as nata de coco, with an oxygen scavenger system in a multilayer structure. In addition, the relationship between microstructure, mechanical properties, and oxygen barrier capability in such systems has not yet been comprehensively explained; further studies are needed. To the best of our knowledge, no study has systematically integrated MCC derived from bacterial cellulose (nata de coco), antioxidant-based oxygen scavenger BHT, and multilayer architecture to elucidate the structure, function, and permeability relationship in the PLA system.

Based on these considerations, this study aims to develop and characterize biodegradable PLA-based plastic with the addition of MCC from nata de coco and BHT as an oxygen scavenger in a multilayer system. This study specifically evaluates the relationship between material structure, mechanical properties, and the resulting oxygen permeability.

The novelty of this work lies in the integrated approach combining natural-source MCC, antioxidant-based oxygen scavengers, and multilayer architecture within a single system, which has not been systematically explored in previous studies. Supported by bibliometric insights highlighting the lack of such integration, this study addresses a critical research gap in sustainable packaging materials. Furthermore, this research contributes to sustainable development goals (SDGs) by promoting biodegradable materials (SDG 12), reducing environmental impact (SDG 13), and enhancing food preservation through active packaging

systems (SDG 2). The contribution of this research is expected to provide new insights into the synergy between cellulose fillers and active agents in biodegradable packaging, as well as to serve as a foundation for the development of high-performance, sustainable active packaging for food applications.

## 2. METHODS

### 2.1. Materials

The equipment used in this study included a stirring rod, glass bottle, desiccator, beaker, drying oven, glass plate/mold, volumetric pipette, cutter knife, analytical balance, storage container, micropipette, tips, hot plate, stirrer, Erlenmeyer flask, DSH-10 moisture analyzer, oven, tension testing device, thermogravimetry apparatus, Fourier Transform Infrared Spectrometer (FT-IR), and Scanning Electron Microscope (SEM). The materials used in this research are distilled water, MCC powder from hydrolyzed nata de coco, Avicel PH 102 MCC, BHT, chloroform, barium chloride ( $\text{BaCl}_2$ ), sodium chloride ( $\text{NaCl}$ ), activated carbon, iron powder, PLA, Polyethylene Glycol 400 (PEG-400), aluminum foil, plasticine, compost soil, and labels

### 2.2. Bacterial Cellulose Production

Bacterial cellulose production follows the method by [10]. The process, shown in **Figure 1**, is carried out using coconut water from optimally mature coconuts (11–12 months old), which is then left to stand for 5 days to lower the pH. The coconut water is boiled and supplemented with a small amount of sucrose at 5% (w/v), acetic acid at 1% (v/v), and a nitrogen source at 0.5% (w/v), such as ammonium sulfate and yeast extract. Next, 1,200 mL of the hot coconut water is poured into a container measuring 19×16.5×9 cm. The surface of the container is then covered with aluminum foil and left for 24 hours, after which it is inoculated with a 10% (v/v) starter culture of *Acetobacter xylinum*. Thereafter, fermentation is carried out for 4–14 days at a temperature of 28–30°C to form a nata pellicle or cellulose membrane on the surface of the medium.

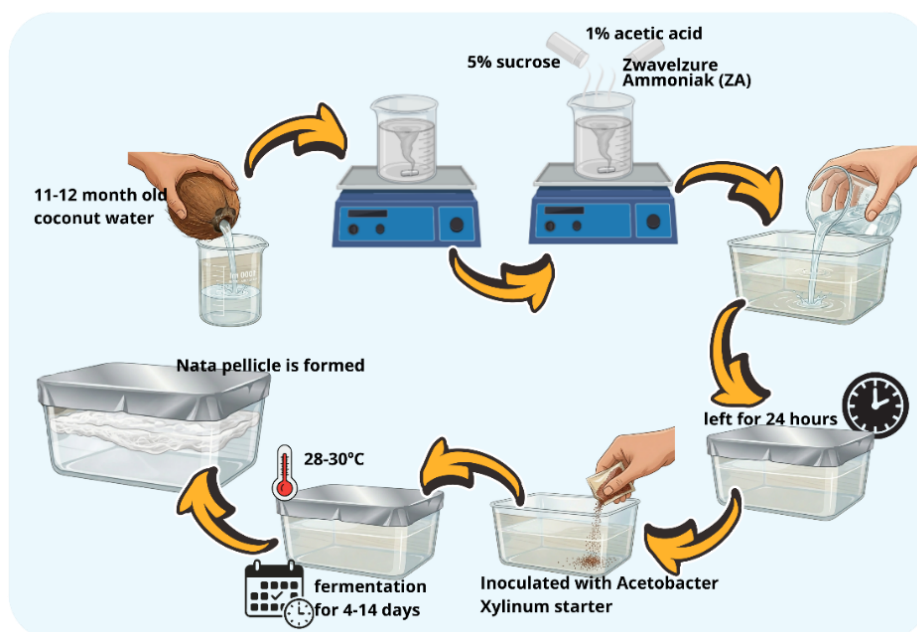


**Figure 1.** Mechanism of bacterial cellulose production by *Acetobacter xylinum*.

### 2.3. Bacterial Cellulose Purification

The purification of bacterial cellulose follows the method by [10]. Purification process, as shown in **Figure 2**, is carried out by removing the cellulose membrane from the fermentation medium, rinsing it with running water, and then soaking it for 2 days with periodic water changes. Next, the cellulose is soaked in 70% alcohol for 1 minute, then heated in distilled water up to 100°C for 20 minutes, and reheated in a 5% NaOH solution at 100°C for 60 minutes to remove residual bacterial cells and substrate attached to the cellulose layer. After that, the cellulose is rinsed with running water and soaked in water that is periodically replaced for 24 hours until the pH reaches 7. The purified cellulose will appear transparent.

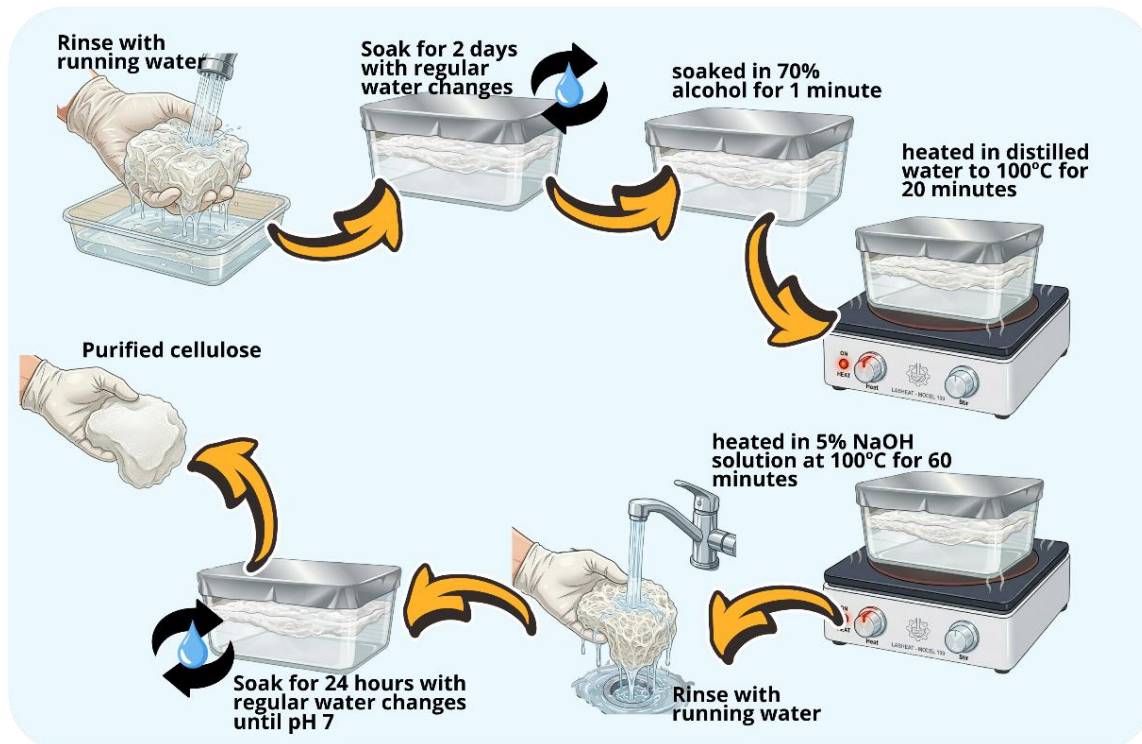


**Figure 2.** Mechanism of bacterial cellulose purification.

### 2.4. Production of Bacterial Cellulose Powder

The purified bacterial cellulose, as shown in **Figure 3a**, will be pressed with a hydraulic press to reduce water content and speed up the drying process. The nata is dried using an oven at a temperature between 30 and 35 °C. Drying at temperatures higher than 35 °C will make the cellulose less reactive. The dried nata is then reduced in size by cutting it into small pieces and grinding it with a 40-mesh hammer mill.

### 2.5. Production of Microcrystalline Cellulose Powder

Production of microcrystalline cellulose, as shown in **Figure 3b**, bacterial cellulose powder is boiled in hot water, then the residue is collected and boiled with 2% NaOH at 80°C for 30 minutes. After that, the residue is washed with distilled water until the pH reaches 6-7, then soaked in 18% NaOH.

This residue is then oven-dried to produce alpha-cellulose, after which the cellulose powder is hydrolyzed with 2.5 N hydrochloric acid by boiling for 15–20 minutes, and then the residue is neutralized by rinsing with distilled water. After that, the residue is dried and ground to produce microcrystalline cellulose [11].

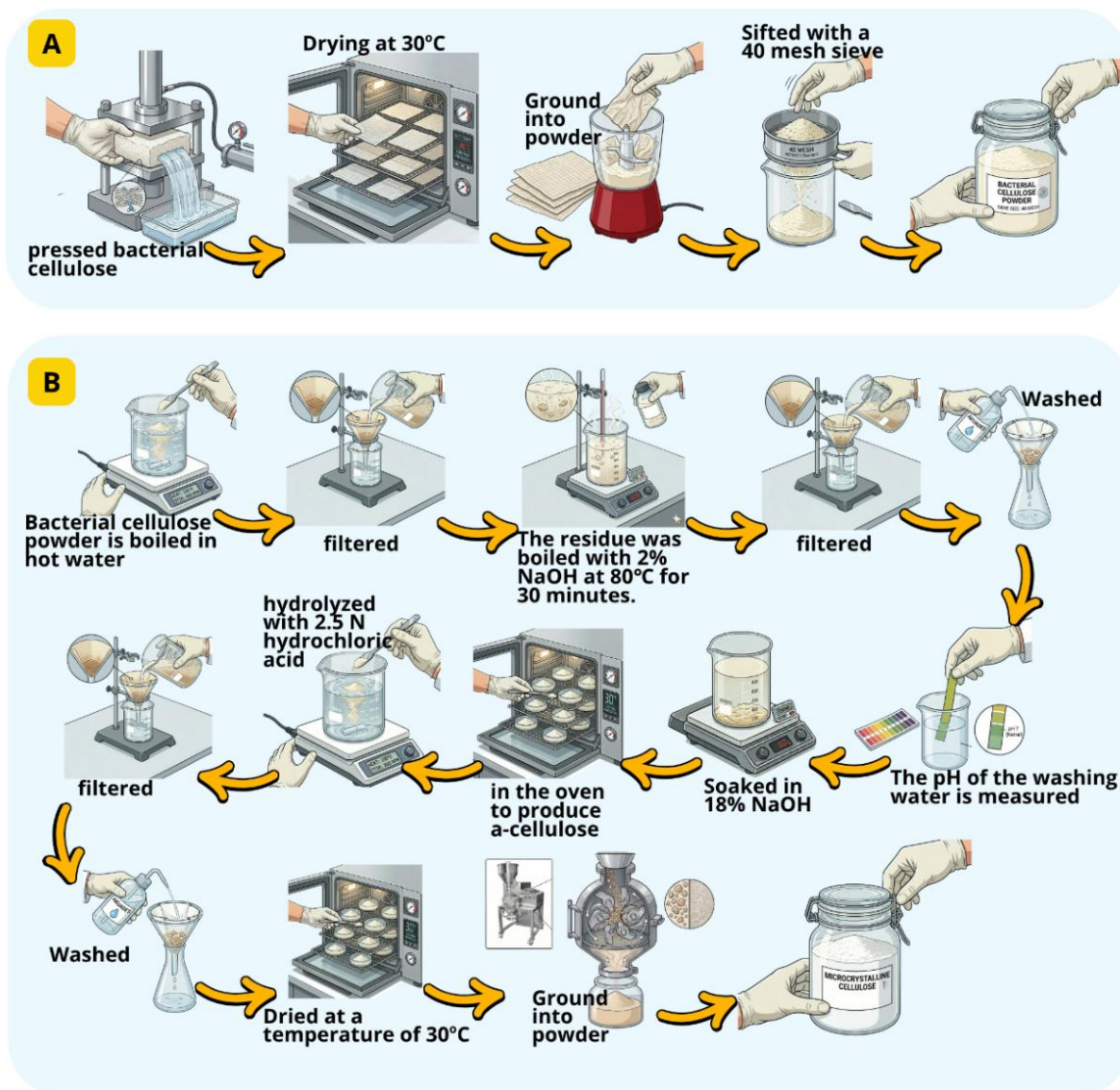


**Figure 3.** Mechanism of bacterial cellulose powder production (a) and microcrystalline cellulose powder production (b).

## 2.6. Production of Oxygen-Absorbing Biodegradable Plastic

The process of making oxygen-absorbing biodegradable plastic, as shown in **Figure 4**, involves mixing PLA at 7% of the amount of chloroform used, that is, 10.5 g of PLA in 150 mL of chloroform, using a stirrer at a speed of 750 rpm at a temperature of 25°C. Next, MCC powder is added according to the treatment levels 20, 10, and 0% of the amount of PLA used, which equals 2.1, 1.05, and 0 g of MCC while continuing to stir.

Once mixed, 5% PEG-400 by PLA, which is 0.525 ml, is dropped in, and after it dissolves, 10% of the PLA amount of Butylated hydroxytoluene (BHT), totaling 1.05 g, is added. Once dissolved, the solution is poured onto square glass plates at a rate of 10 g per layer, then leveled, air-dried, and the process is repeated until three layers are formed. The result is then left to dry for 24 hours at room temperature.

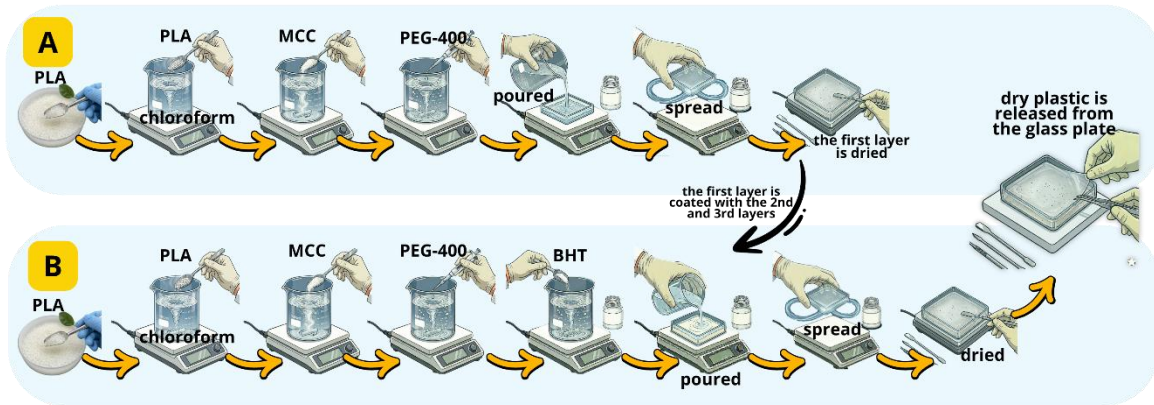


**Figure 4.** Scheme for producing the first layer (outer) (a), second, and third layers (active and inner) (b) of oxygen-absorbing biodegradable plastic with butylated hydroxytoluene.

## 2.7. Experimental Design

This study used a two-stage experimental design to systematically evaluate the effect of MCC incorporation on the performance of biodegradable films. In Stage I, two types of MCC (MCC Avicel ph 102 and MCC derived from nata de coco) were incorporated into the film matrix at three different concentrations (0, 5, and 10%, w/w). These initial formulations were primarily evaluated based on their morphological characteristics using a scanning electron microscope (SEM) to identify structural homogeneity, filler dispersion, and the presence of microvoids or agglomerations. Based on the results of the SEM evaluation, the selected formulation was then tested further (stage II).

## 2.8. Experimental Procedures

### 2.8.1. Morphology Analysis

Morphological analysis using SEM is carried out by cutting the sample to fit the specimen holder size (between 0.5 and 1 cm), then attaching it to the specimen holder using carbon double tape with the cross-section facing vertically upwards toward the objective lens. Since biodegradable plastic samples are non-conductive, the samples are coated with a conductive inert metal, specifically gold, which acts as a conductor for 30 seconds to 2 minutes. After that, the sample is placed on the stage block and tested with SEM at a voltage of 5-15 kV and a magnification of 100-5000 times. The SEM results are presented in three-dimensional images, where the morphology and topography are observed.

### 2.8.2. Thickness Test

The plastic thickness testing stage is carried out by cutting plastic samples to a size of 10 x 10 cm. The thickness of the plastic is then measured using a caliper with an accuracy of 0.01 mm at 5 different points. The thickness of the plastic is obtained from the average result calculated using the following equation (1).

$$\text{Plastic thickness (m)} = \frac{\sum \text{plastic thickness}}{n} \quad (1)$$

### 2.8.3. Tensile Strength Test

The tensile strength test for biodegradable plastic was carried out using a tension testing device. The bioplastic sample was cut to a size of 1 x 15 cm, then clamped 1.5 cm from both ends along its length. Next, the sample was tested using the tension testing device. The initial length was recorded, then the device was started by pressing the start knob, after which it

pulled the plastic sample until it broke. The tensile force and the length of the plastic after breaking were then recorded. The tensile strength value can be calculated using the following equation (2).

$$s \text{ (MPa)} = \frac{F_{max}}{A} \quad (2)$$

where  $s$  is the tensile strength (MPa);  $F_{max}$  is the Force (N); and  $A$  is the cross-sectional area (thickness x sample width) ( $\text{mm}^2$ ).

#### 2.8.4. Elongation Break Test

The elongation or extension testing stage for biodegradable plastic is carried out using a tension testing device in the same way as the tensile strength test, that is, the initial length is recorded, then the device is activated by pressing the start knob, and it will pull the plastic sample until it breaks. The tensile force and the length of the plastic after breaking are then recorded. The elongation value is expressed as a percentage using the following equation (3).

$$\varepsilon \text{ (\%)} = \frac{\Delta l}{l_0} \times 100\% \quad (3)$$

where  $\varepsilon$  is the Elongation/stretching (%),  $\Delta l$  is the Increase in length(mm), and  $l_0$  is the initial length of the measured material (mm).

#### 2.8.5. Young's Modulus Test

The elasticity testing stage for biodegradable plastic is carried out using a Tension testing device in the same manner as the tensile strength test, where the initial length is recorded, then the device is turned on by pressing the start knob, and the device will pull the plastic sample until it breaks. The tensile force and the length of the plastic after breaking are then recorded. The modulus of elasticity is obtained using the formula comparing the tensile strength to the elongation, as follows (see equation (4)).

$$\gamma = \frac{s}{\varepsilon} \times 100\% \quad (4)$$

where  $\gamma$  is the modulus of elasticity (MPa);  $s$  is the tensile strength/stress (MPa);  $\varepsilon$  is the elongation/stretching (%).

#### 2.8.6. Oxygen Permeability Test

The oxygen permeability level of biodegradable plastic is measured using the Deoxidizing Substance Adsorption method, which refers to the iron oxidation mechanism, as described in the literature [12]. The process begins by preparing a glass bottle containing 3 g of a deoxidizing agent composed of sodium chloride, activated carbon, and reduced iron powder in a ratio of 1.5: 1: 0.5, respectively. Next, the mouth of the bottle is wrapped with a bioplastic sample measuring 6 x 6 cm, then sealed tightly with plasticine, after which the bottle is weighed to determine its initial weight. The bottle is then placed in a desiccator containing a saturated barium chloride solution at the bottom, maintaining the RH at 90% at a temperature of 25 °C for 48 hours. The oxygen permeability value is calculated using the following equation (5).

$$\text{Oxygen permeability} = \frac{M_f - M_i}{t - A} \quad (5)$$

where  $M_f$  is the final bottle weight after being stabilized for 48 hours;  $M_i$  is the initial bottle weight;  $t$  is the equilibrium time (s); and  $A$  is the effective plastic area ( $\text{mm}^2$ ).

### 2.8.7. Chemical Structure

Analysis of functional groups using FT-IR is carried out by cutting the sample to the size of the lens, then placing it on the sample holder, facing the infrared beam. Next, the spectrum formed between the wavenumber and transmittance is observed, and the functional groups present in the plastic material are identified.

### 2.8.8. Biodegradability Test

Biodegradability testing is carried out using the soil burial method. The biodegradable plastic samples are cut into 2 x 2 cm pieces and then buried in compost soil at a depth of 7.5 cm. The samples are then incubated at room temperature for 25 days, with observations made every two days.

Afterward, the samples are cleaned of any adhering soil and weighed. The degree of biodegradability is determined by the loss in sample weight, calculated by weighing the samples before and after burial. The percentage of weight loss is calculated using the following equation (6).

$$\text{Weight loss (\%)} = \frac{B_o - B_f}{B_o} \times 100\% \quad (6)$$

where  $B_o$  is the initial weight of the sample before planting, and  $B_f$  is the sample weight after planting.

### 2.8.9. Moisture Content Test

Moisture content analysis was carried out using a DSH-50-1 moisture analyzer with an accuracy of 0.001g, which had been previously calibrated. A 3g sample was weighed and placed on the moisture analyzer pan, then the device cover was closed. Next, press the test button to start the measurement until the device emits a beeping sound, indicating that the moisture content value on the monitor has stabilized. Then, press the test button again to stop the device. After that, record the moisture content value displayed on the monitor.

## 3. RESULTS AND DISCUSSION

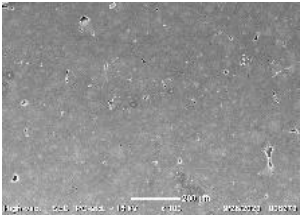
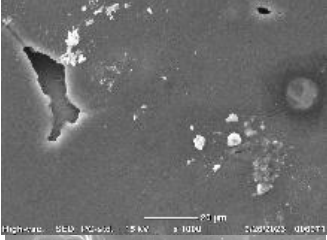
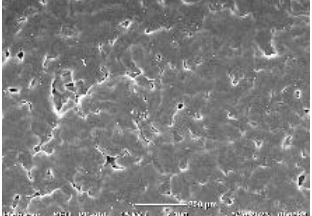
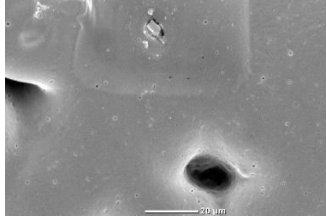
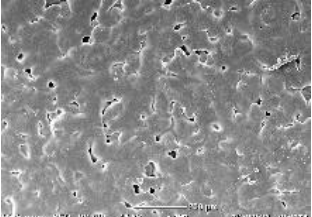
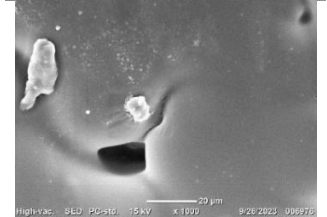
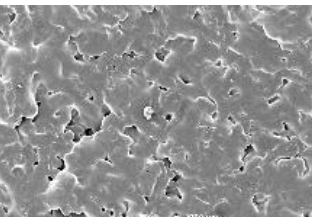
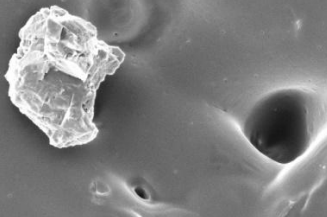
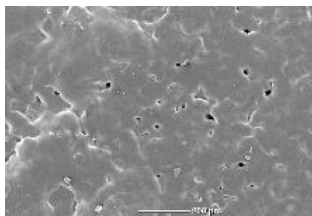
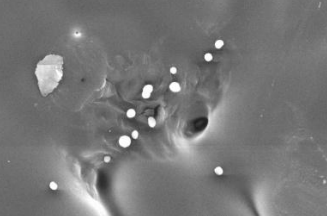
### 3.1. Morphology of Plastic Biodegradable

The principle is that electrons interact with the atoms in the sample, and the resulting signals can be detected and interpreted as high-resolution images. The SEM images revealed that MCC dispersion varied, depending on concentration and source. Based on **Table 1**, the result of SEM testing at magnifications of 100-3000x on biodegradable plastic samples with the addition of MCC powder at concentrations of 0, 10, and 20%, differences were observed in the surface structure in the form of matrix bonds, voids, and reinforcement. Voids are cavities formed due to imperfections in the bonding matrix, while reinforcement refers to particles that serve as fillers and strengthen the matrix structure [13].

When observing the morphology of the plastic samples, it can be seen that increasing the concentration of MCC powder results in a more complex and thicker structure. This is evident in the plastic treated with 0% MCC, which shows tears in the matrix.

With the addition of MCC (10%), the surface structure tends to have more voids (gaps/pores) and less reinforcement in its matrix compared to the 20% treatment. The addition of MCC powder functions as an adhesive and increases the tensile strength of the plastic, making it more durable and less prone to breaking [14].

**Table 1.** SEM results of biodegradable plastic MCC nata de coco and MCC avicel ph 102 with 0, 10, and 20% formulations.

FORMULATION	SEM IMAGES	
A0B0 MCC (0%)		
A1B1 MCC avicel pH 102 (10%)		
A2B1 MCC nata de coco (10%)		
A1B2 MCC avicel pH 102 (20%)		
A2B2 MCC nata de coco (20%)		

In addition, when comparing the SEM results of MCC nata de coco with MCC Avicel PH 102, there is a difference where MCC Avicel PH 102 (20%) shows a less organized matrix structure and tends to have more voids. This result is because nata de coco tends to be rich in fiber and pure cellulose compared to plant-derived cellulose [15].

Based on these observations, it can be concluded that the addition of MCC nata de coco powder as a filler and reinforcement material can provide a better effect on the mechanical properties of biodegradable plastic and oxygen barrier performance, specifically its tensile strength, making the resulting plastic less prone to breaking or damage. This is in line with the fact that a higher number of void defects (cavities) in a matrix structure tends to increase the brittleness of plastic materials [13].

### 3.2. Advanced Characterization of Selected Film

The results of tests conducted in the first stage, which identified the best treatment as the addition of MCC nata de coco (20%), were followed by a second stage involving physical and chemical testing of the resulting biodegradable plastic. The results can be seen in **Table 2**.

**Table 2.** Results of physical and chemical properties tests of biodegradable plastic.

PARAMETER	VALUE
Thickness (mm)	$0.33 \pm 0.02$
Tensile strength (MPa)	$5.27 \pm 0.28$
Elongation break (%)	$0.91 \pm 0.015$
Modulus of Elasticity (MPa)	$581.40 \pm 33.466$
Oxygen Permeability( $10^{-10}$ g / m s Pa)	$4.10 \pm 0.49$
Moisture Content (%)	$8.0 \pm 0.45$

#### 3.2.1. Thickness

Thickness testing on biodegradable plastic is used to determine the characteristics of biodegradable plastic that affect its use in packaging a product. The thickness of a plastic can influence the oxygen permeability level of the plastic as a product packaging material. Generally, the thicker the plastic, the lower its oxygen permeability [16]. In addition, the thickness of a plastic will also affect other characteristics of the plastic, such as tensile strength and elongation [17]. Based on **Table 2**, it can be seen that the measurement results for the thickness of biodegradable plastic with the addition of 20% MCC powder yielded a thickness value of  $0.33 \pm 0.02$  mm. These measurement results do not meet the standards when compared to the Japanese Industrial Standard (JIS), that is,  $< 0.25$  mm [17]. Meanwhile, when compared to the American Society for Testing and Materials (ASTM) D882-12 standard, which is in the range of 0.1-0.5 mm, the results obtained meet the established thickness standard. The thickness level of this biodegradable plastic is influenced by the addition of MCC powder as a filler and reinforcement material, as well as the application of a multilayer (3-layer) structure to the plastic, as shown in **Figure 5**.

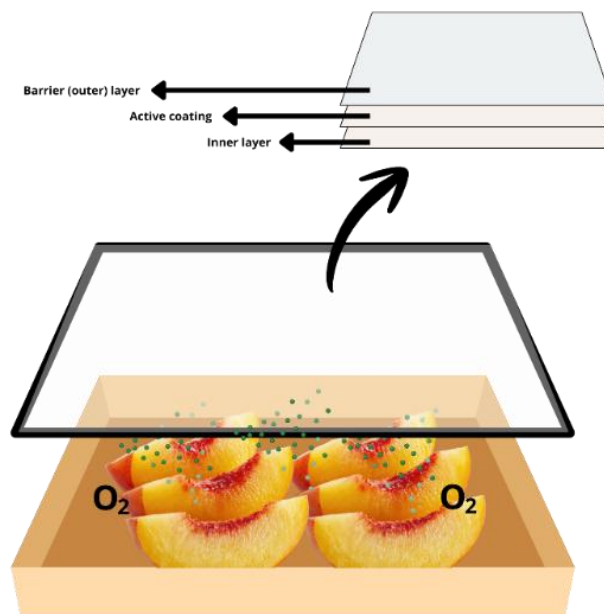


**Figure 5.** Prototype plastic biodegradable multilayer.

The multilayer application is carried out with three layers on the plastic, with the outermost layer not containing BHT, while the second and third layers, which are in contact with the food, are added with BHT as the active ingredient. This multilayer application is intended to enable the plastic to exhibit better barrier properties. In addition, the multilayer method allows for the use of active agents in the form of oxygen absorbers in the plastic layers, ensuring that only the oxygen inside the packaging is absorbed. This is consistent with the statement. Combining several layers with different properties, multilayer packaging can achieve better barrier performance [6].

### 3.2.2. Tensile Strength

Tensile strength testing aims to determine the effect of MCC powder on the characteristics. Based on **Table 2**, it can be seen that the tensile strength measurement results for biodegradable plastic with the addition of MCC powder have a tensile strength value of  $5.27 \pm 0.28$  MPa. These results are in accordance with the standard when compared to the standard, namely  $>3.92$  MPa; thus, biodegradable plastic with the addition of MCC powder meets the tensile strength standard. The resulting tensile strength value is influenced by the addition of MCC powder, which acts as a filler and reinforcement for biodegradable plastics, which will increase strength. This is in accordance with the statement in some papers that the addition of fillers and reinforcements to the matrix structure provides good adhesive properties [13].

However, based on **Table 3**, the results obtained are still far behind compared to several polymers with the addition of MCC powder. This indicates that the effectiveness of SM is greatly influenced by matrix compatibility, preparation methods, and filler distribution [18]. Studies with good dispersion and interfacial interaction result in high TS, while systems dominated by elastic matrices, such as starch, show low TS.

In the results of this study, the TS value of  $5.27 \pm 0.28$  MPa is considered relatively low compared to the literature, indicating that although MCC was added, its reinforcing effect was not yet optimal. This is likely due to the non-homogeneous dispersion of MCC leading to agglomeration, weak interfacial adhesion between SM (hydrophilic) and PLA (hydrophobic), and a lack of compatibilizers that could enhance interphase interaction [19]. Thus, although MCC powder has the potential to be used as a filler that can improve tensile strength, the results of this study show that without formulation optimization, this improvement is not fully achieved.

### 3.2.3. Elongation Break

Elongation plays an important role in indicating the extent of plastic deformation without damage when used as packaging. Based on **Table 2**, it can be seen that the elongation value of biodegradable plastic with the addition of 20% MCC powder is  $0.91 \pm 0.015\%$ . This result is far below the elongation standard for plastics according to JIS K 7113:2019, which is  $>50\%$  [17]. The results of this test also do not meet the standards, as the minimum value of plastic elongation is 10%. This is due to the decreased ductility of biodegradable plastic after the addition of MCC powder, which increases the stiffness of the existing biodegradable plastic. In addition, the amount of PEG added can affect the hardness level if it is not proportional to the weight of the polymer used. This aligns with the fact that the amount of PEG-400 used is only 5% of the total polymer weight. This is supported by the statement that in the production of biodegradable plastic, PEG 400 is used at 14% of the amount of polymer used [20].

Data in **Table 3** shows a consistent trend, where packaging with a high MCC powder content or strong structure tends to have a low Elongation break (EB), while packaging with a more flexible starch matrix has a high EB value of up to 59.80%. In this study, the EB value obtained was very low, at  $0.91 \pm 0.015\%$ , indicating that the film is extremely brittle. This value is even lower than most previous studies, indicating that the addition of MCC significantly reduces elasticity without being offset by the matrix's flexibility. This discrepancy may be caused by an uneven distribution of MCC, creating points of stress concentration, as well as a lack of effective molecular interaction between MCC and PLA [21]. Therefore, although the decreasing trend of EB is in line with theory, the very low values in this study highlight the critical trade-off between oxygen barrier enhancement and mechanical flexibility, which remains a major challenge in biopolymer-based packaging systems.

**Table 3.** Physical characteristics of plastic with the addition of microcrystalline cellulose.

FILM PREPARATION	MCC LOADING RANGE	TS (MPA)	EB (%)	YM	REF.
Casting; gel concentrated and air-dried	Multiple ratios	$48.4 \pm 2.9$	$7.8 \pm 0.8$	$2.1 \pm 0.1$ GPa	[5]
MCE/SA dissolved in toluene, sprayed onto paper; PHMG grafted	Not explicitly	16	3.2	nd	[25]
Casting onto PET films, dried at 40 °C for 24 h	4.5 g/100 mL	16.58	17.3	nd	[26]
MCC mixed with PLA in dichloromethane; automatic coating machine	0–12 wt%	6.2	nd	nd	[27]
Solvent casting; film thickness	0–60 wt% based on starch	1.93	59.80	0.22	[28]
Solution casting with PVA	0.1–5 wt%	$31.7 \pm 2$	9.1% decrease from control	nd	[29]
Sonification of MCC solution	0.5% w/w	$11.24 \pm 0.68$	$31.0 \pm 3.88$	nd	[30]
Integration of MCC into PLA	20% b/v	$5.27 \pm 0.28$	$0.91 \pm 0.015$	$581.40 \pm 33.47$ MPa	This study

\*nd = No data; TS = Tensile strength; EB = Elongation break; YM = Young's modulus

### 3.2.4. Young's Modulus

The modulus of elasticity is the measure of a material's stiffness, indicating how much a material can undergo elastic deformation when subjected to a certain force. The modulus of elasticity is also defined as the ratio between the stress and strain experienced by the material [22]. The higher the modulus value, the more rigid the plastic material becomes, and the less likely it is to deform [23]. As shown in **Table 2**, the results of the elasticity modulus test show that the elasticity modulus value of the biodegradable plastic is  $581.40 \pm 33.466$  MPa. This result indicates that the biodegradable plastic is rigid when compared to the standard elasticity modulus according to JIS, which is at least 0.35 MPa [24]. This is influenced by the

low strain values in the plastic, which are caused by an imbalance between the concentration of MCC powder as a reinforcement material and PLA as a polymer relative to the amount of plasticizer used, namely PEG400, which tends to be low [20].

### 3.2.5. Oxygen Permeability

Oxygen permeability is the ability of a material, in this case plastic, that allows oxygen molecules to pass through it [31]. This affects the performance and durability of the product, especially when used in food packaging. Plastics with low oxygen permeability can slow down the oxidation process, resulting in longer-lasting packaged products. Based on the results in **Table 2**, the oxygen permeability value of biodegradable plastic with a PLA polymer matrix and the addition of 20% MCC powder and 10% BHT has a value  $4,10 \pm 0,49 \times 10^{-10}$  g /m s Pa.

Several test results of plastics with similar polymers, namely PLA, showed an oxygen permeability value of  $5.0 \times 10^{-7}$  g/m s Pa. The permeability value for synthetic plastic LDPE is in the range of  $1.47 \times 10^{-12} - 9.79 \times 10^{-13}$  g/m s Pa [25]. Different from HDPE plastic, which has a value of  $1.011 \times 10^{-13} - 4.47 \times 10^{-13}$  g/m s Pa [32].

Based on these values, the results obtained, when compared to similar polymers such as PLA, show better oxygen permeability, but still do not reach the permeability levels of synthetic plastics like LDPE and HDPE. This can be attributed to the addition of MCC, which enhances the density of the biodegradable plastic structure and creates a barrier to oxygen entry. In addition, the addition of BHT also contributes to absorbing oxygen content, thus reducing the rate of oxygen diffusion and resulting in a low oxygen permeability value [31]. The mechanism of BHT in oxygen absorption can be seen in the following figure.

Based on **Figure 6**, it can be seen that the BHT compound will release a labile hydrogen (which is easily donated to free radicals), with the labile hydrogen located on the hydroxyl group (-OH). The hydroxyl group (-OH) acts as a donor of labile hydrogen, which will later be donated to neutralize free radicals, turning them into more stable radicals.

More stable radicals are not reactive toward oxygen, thus reducing the possibility of generating more free radicals [33]. Thus, BHT plays a role in reducing the concentration of oxygen available for oxidation reactions, thereby slowing down the deterioration process of food products.

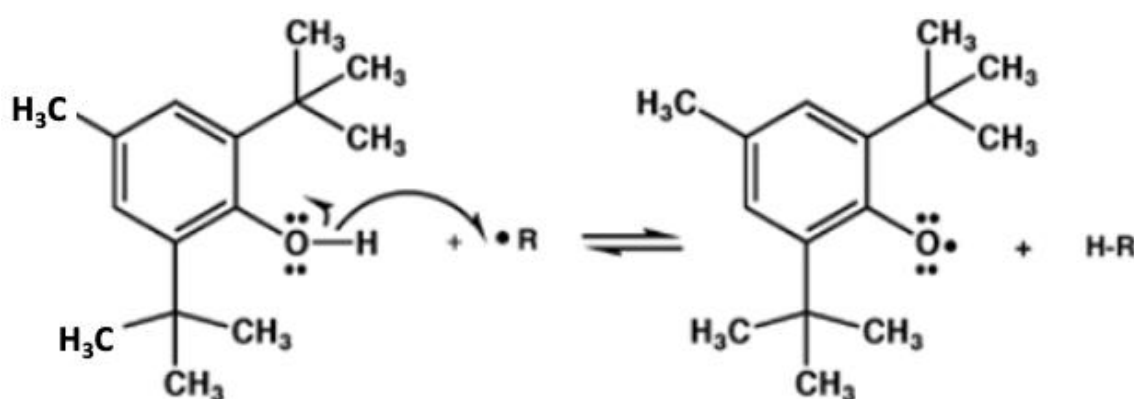


**Figure 6.** Oxidation reaction of BHT through the hydrogen donor mechanism. BHT changes into the BHT radical.

### 3.2.6. Chemical Structure

Fourier Transform Infrared (FT-IR) mechanism involves measuring the interaction between infrared radiation and matter, specifically the absorption of light at certain wavelengths [34]. Data collected as a function of time is then converted into a frequency spectrum using the Fourier transformation, enabling the identification of chemical bonds and molecular structures in the sample.

As shown in **Figure 7**, the FTIR testing results on the MCC 20% Plastic sample produced several peaks. The first peak, in the 1700-1800 range with a sharp downward and narrower shape, indicates the presence of a carbonyl group (C=O) in the compound. This group is formed in organic compounds containing esters and carboxylic acids [35]. The second and third peaks fall within the fingerprint region. The second absorption band is found at the peak of 1180, where the range of 1000-1300 indicates the presence of a C-O functional group.

This group is formed in organic compounds containing esters and alcohols. The C-O functional group, which is characteristic of ester compounds, indicates that the film layer of the biodegradable plastic is hydrophilic, making it easily degradable [36]. The third peak has an absorption band at 1080, where this absorption band lies within the range of 1070-1140, indicating the presence of an ether compound with a C-O-C group [37]. The C-O-C functional group in ether compounds plays a role in increasing tensile strength and elastic modulus; however, the ability to stretch decreases [38].

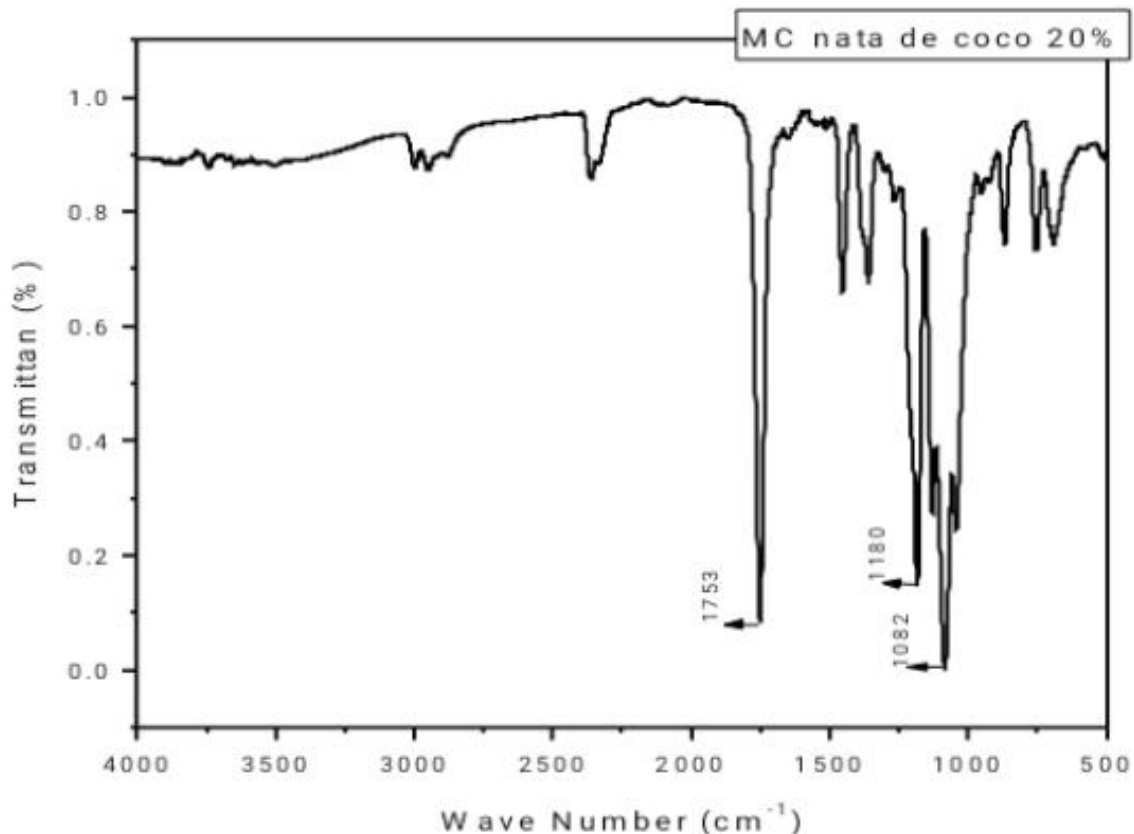


**Figure 7.** FTIR spectrum of biodegradable MCC nata de coco plastic.

### 3.2.7. Biodegradability

Biodegradation is the natural process of breaking down organic materials into simpler compounds through the action of microorganisms. The ability of a material to decompose is referred to as biodegradability. Biodegradability tests on biodegradable plastics are conducted to determine the degree of plastic material decomposition, thereby assessing their role in reducing the negative impact of conventional plastics on the environment.

The biodegradation process of packaging in the environment occurs through chemical decomposition, resulting in polymers with lower molecular weights by breaking molecular bonds [39]. The following are the results of the biodegradability level test for biodegradable plastic. Based on the analysis of variance, the interval of days has a significant effect at the 5% level ( $p < 0.05$ ) on the biodegradability level of the biodegradable plastic.

Based on **Figure 8**, the biodegradation rate was found to be 28.86% over 25 days, with the highest degradation rate occurring on the 25th day at 9%. The test results show that the level of biodegradation is in good accordance when compared to biodegradable plastics using similar polymers, which is  $>25\%$  within a period of 25 days [40].

In addition, these results show good conformity when compared to the ASTM D6400-12 standard, which requires a biodegradation rate of 90% within 180 days under composting conditions. These results are influenced by the nature of PLA, which is easily decomposed through the process of hydrolysis by microorganisms [41]. In addition, the addition of plasticizers also helps to bind moisture content, thereby facilitating the hydrolysis process of plastic by microorganisms.

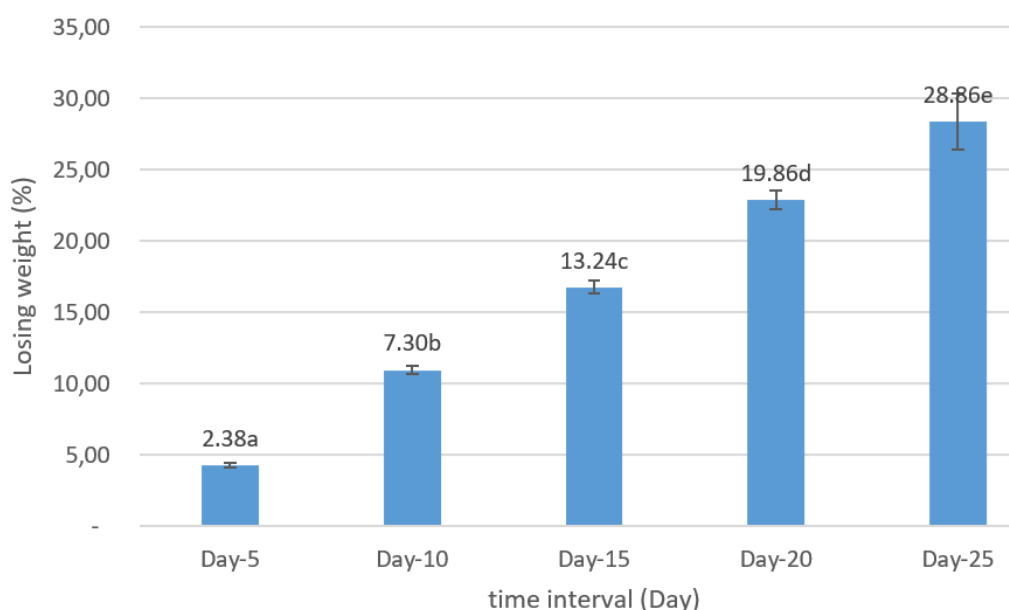


**Figure 8.** The biodegradability levels of biodegradable plastics.

### 3.2.8. Moisture Content

Moisture content in biodegradable plastics can affect the physical and mechanical properties of the plastic, especially when used for packaging food products. Plastic with too low a moisture content becomes brittle, while too high a moisture content can accelerate the biodegradation of the plastic and also affect the shelf life of the packaged food products [42]. Based on **Table 2**, the moisture content obtained was  $8.0 \pm 0.45\%$ . When compared to the

moisture content of biodegradable plastic made with a combination of Walur starch and glycerol, it ranges from  $9.45 \pm 2.89\%$  [43].

In addition, the combination of cellulose acetate with PEG-600 resulted in a water content of  $10.23 \pm 0.45\%$ , with the highest water content found in the plasticizer formulation at 50% [40]. The greater concentration of plasticizer added resulted in higher water content. This is because the plasticizer functions to bind the water content [43].

Thus, the higher the water content in biodegradable plastic, the greater its potential to accelerate biodegradation, which is influenced by the concentration of plasticizer used. This is in accordance with some papers that the plasticizer binds water during the polymerization process, making the resulting biodegradable plastic softer and easier to degrade.

### 3.2.9. Bibliometric Trends and Relevance to Sustainable Development Goals

A bibliometric analysis was conducted to examine the global research trends in food packaging, as illustrated in **Figure 9**. The data, obtained from a TITLE-ABS-KEY query, show a significant and continuous increase in the number of publications over time, particularly after the early 2000s.

The sharp rise in recent years reflects the growing scientific and industrial interest in advanced packaging technologies, driven by concerns related to food safety, shelf-life extension, and environmental sustainability. The exponential growth of publications indicates that food packaging has become a critical research area, especially with the increasing demand for sustainable and functional materials.

The rapid expansion of research output is closely associated with the development of biodegradable polymers, active packaging systems, and oxygen-scavenging technologies. These advancements aim to address major challenges such as plastic waste accumulation and food spoilage. In particular, the integration of structural reinforcement materials and active agents within multilayer systems remains an emerging research direction, as highlighted by the relatively limited studies focusing on combined functionalities. This observation supports the identified research gap and justifies the need for developing integrated biodegradable packaging systems.

From a sustainability perspective, the increasing research trend strongly aligns with several SDGs. Specifically, SDG 12 (Responsible Consumption and Production) is addressed through the development of biodegradable materials that reduce reliance on conventional plastics. SDG 13 (Climate Action) is supported by minimizing environmental impact and promoting eco-friendly material design. In addition, SDG 2 (Zero Hunger) is indirectly targeted through the enhancement of food preservation using oxygen-scavenging packaging systems that extend shelf life and reduce food waste.

Therefore, the bibliometric findings not only demonstrate the growing importance of food packaging research but also emphasize the urgency of developing innovative, sustainable, and multifunctional materials. The present study contributes to this evolving field by integrating structural reinforcement and active functionality in a multilayer biodegradable system, thereby addressing both technological challenges and global sustainability goals. Finally, this study adds new information regarding SDGs, as reported elsewhere [44].

TITLE-ABS-KEY ( food AND packaging )

63,453 document results

Select year range to analyze: 1935 to 2025 Analyze

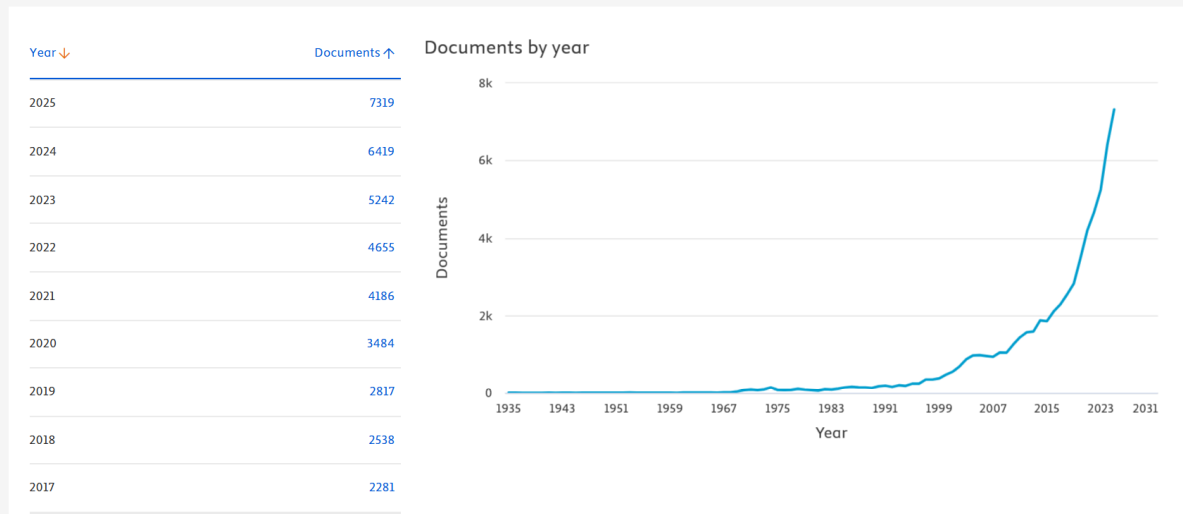


**Figure 9.** Bibliometric analysis of global research trends in food packaging based on TITLE-ABS-KEY query, showing the annual number of publications over time. Data were obtained from the Scopus database in April 2026.

#### 4. CONCLUSION

This study presents a bibliometric and experimental investigation of multilayer oxygen-scavenging biodegradable polylactic acid films reinforced with microcrystalline cellulose and butylated hydroxytoluene. The results demonstrate that the integration of structural reinforcement and active functionality enhances material performance, particularly in improving barrier properties while maintaining mechanical integrity. Bibliometric findings confirm the growing research interest and highlight the need for integrated multifunctional systems. The novelty lies in combining natural-source cellulose, antioxidant-based oxygen scavengers, and multilayer architecture within a unified structure–property–function framework. This approach supports sustainable food packaging development and contributes to SDGs, particularly responsible production, climate action, and food preservation.

#### 5. ACKNOWLEDGMENT

We would like to thank all parties who have contributed to the completion of this research. This research was supported by the RIIM LPDP and BRIN Grants, with grant numbers 113/IV/KS/07/2025 and 3259/UN4.1.7/PT.01.03/2025.

#### 6. AUTHORS' NOTE

The authors declare that there is no conflict of interest regarding the publication of this article. The authors confirmed that the paper was free of plagiarism.

#### 7. REFERENCES

- [1] Patel, C. J., Kansagara, R. H., Modi, D. V., Dudhat, N. J., Sojitra, K. H., and Babaria, D. M. (2024). Microbes breaking down plastic: Insights for sustainable waste management. *Nature Environment and Pollution Technology*, 23(3), 1717-1722.
- [2] Chen, J., Long, Z., Wang, J., Wu, M., Wang, F., Wang, B., and Lv, W. (2017). Preparation and properties of microcrystalline cellulose/hydroxypropyl starch composite films. *Cellulose*, 24(10), 4449-4459.

- [3] Yang, S., Che, R., Chen, J., He, Z., Lai, T., Liang, Y., and Bian, X. (2024). A feasible way to modify microcrystalline cellulose powder and its reinforcing effect for NBR composites. *Polymer Composites*, 45(5), 4709-4.
- [4] Huo, Y., Zhu, H., and He, X. (2022). Study of butylated hydroxytoluene inhibiting the coal oxidation at low temperature: Combining experiments and quantum chemical calculations. *ACS Omega*, 7(22), 18552-18568.
- [5] Gong, S., Li, B., Liu, H., Xu, C., Wang, J., Fan, Y., and Yu, J. (2024). Facile preparation of eco-friendly plastic from rosin modified microcrystalline cellulose for food packaging. *Industrial Crops & Products*, 221, 119370.
- [6] Grzebieniarczyk, W., Biswas, D., Roy, S., and Jamróz, E. (2023). Advances in biopolymer-based multi-layer film preparations and food packaging applications. *Food Packaging and Shelf Life*, 35, 101033.
- [7] Yolanda, D. S., Dirpan, A., Nur, A., Rahman, F., and Djalal, M. (2020). The potential combination of smart and active packaging in one packaging system in improving and maintaining the quality of fish. *Canrea Journal: Food Technology, Nutritions, and Culinary*, 3(2), 74–86.
- [8] Yuliana. (2025). Design and development of dragon fruit (*Hylocereus polyrhizus*) peel extract-based freshness indicators for avocado (*Persea americana* Mill) smart packaging. *Respobio Journal: Postharvest Technology and Food Biotechnology*, 1(1), 31–41.
- [9] Kamaruddin, I., Dirpan, A., and Bastian, F. (2021). The novel trend of bacterial cellulose as biodegradable and oxygen scavenging films for food packaging application: An integrative review. *In IOP Conference Series: Earth and Environmental Science*, 807(2), 022066.
- [10] Dirpan, A., Djalal, M., and Kamaruddin, I. (2022). Application of an Intelligent sensor and active packaging system based on the bacterial cellulose of *Acetobacter xylinum* to meat products. *Sensors*, 22(544), 1–15.
- [11] Agustin, N. (2021). Isolasi dan karakterisasi selulosa mikrokristal dari buah nanas (*Ananas comosus* L. Merr.). *Farmaka*, 19(2), 128-135.
- [12] Said, N. S., Olawuyi, I. F., and Lee, W. Y. (2024). Tailoring pectin-PLA bilayer film for optimal properties as a food pouch material. *Polymers*, 16(5), 1–24.
- [13] Hariyanto, A. (2023). Analisis SEM (scanning electron microscope) dan foto mikro pada material komposit serat tangkai jagung dengan matriks plastik polipropilen. *AutoMech: Jurnal Teknik Mesin*, 3(01), 15–22.
- [14] Abdullah, A. H. D., Putri, O. D., Fikriyyah, A. K., Nissa, R. C., and Intadiana, S. (2020). Effect of microcrystalline cellulose on characteristics of cassava starch-based bioplastic. *Polymer-Plastics Technology and Materials*, 59(12), 1250–1258.
- [15] Rini, F., Yulneriwarni, and Sukara, E. (2022). Additional nata de coco on the performance of cassava starch based bioplastic. *Journal of Tropical Biodiversity*, 3(1), 43–51.
- [16] Putra, E. P. D., Thamrin, E. S., and Saputra, H. (2019). Effect of dragon fruit skin extract (*Hylocereus costaricensis*) on bio-plastic physical and mechanical properties of cassava starch and polyvinyl alcohol. *In IOP Conference Series: Earth and Environmental Science*, 258(1), 012047.
- [17] Brilianti, K. F., Ridlo, A., and Sedjati, S. (2023). Sifat mekanik dan ketebalan bioplastik dari *Kappaphycus alvarezii* menggunakan variasi konsentrasi amilum dengan pmlastis gliserol. *Journal of Marine Research*, 12(1), 95–102.
- [18] Jiang, W., Shen, P., Yi, J., Li, L., Wu, C., and Gu, J. (2020). Surface modification of nanocrystalline cellulose and its application in natural rubber composites. *Journal of Applied Polymer Science*, 137(39), 49163.

- [19] Tarawneh, M. A. A., Shahdan, D., and Ahmad, S. H. (2013). Investigation on the effect of NiZn ferrite on the mechanical and thermal conductivity of PLA/LNR nanocomposites. *Journal of Nanomaterials*, 2013(1), 306961.
- [20] Salfitra, M., and Putra, A. (2023). Effect of calcium carbonate (CaCO<sub>3</sub>) additives on the quality of cellulose-based biodegradable plastics bacteria-polyethylene glycol (PEG) of coconut water (*Cocos nucifera*). *Electrolyte*, 2(02), 65-72.
- [21] Simangunsong, D. I., Hutapea, T. H. A., Lee, H. W., and Ahn, J. O. (2018). The effect of nanocrystalline cellulose (NCC) filler on polylactic acid (PLA) nanocomposite properties. *Journal of Engineering and Technological Sciences*, 50(4), 578–587.
- [22] Sulaeman, B. (2018). Modulus Elastisitas Berbagai Jenis Material. *Pena Teknik: Jurnal Ilmiah Ilmu-Ilmu Teknik*, 3(2), 127.
- [23] Sakti, D. I., Setiyana, B., and Tauviqirrahman, M. (2023). Studi perbandingan investigasi modulus elastisitas antara metode uji tarik dengan metode indentasi pada material styrene butadiene rubber 25 (SBR-25). *Jurnal Teknik Mesin*, 11(2), 147-156.
- [24] Desramadhani, R., and Kusuma, S. B. W. (2023). The effect of sorbitol concentration on the characteristics of starch-based bioplastics. *Indonesian Journal of Chemical Science*, 12(2), 130–142.
- [25] Huang, C. H., Wu, J. S., Huang, C. C., and Lin, L. S. (2003). Adhesion, permeability, and mechanical properties of multilayered blown films using maleated low-density polyethylene blends as adhesion-promoting layers. *Polymer Journal*, 35(12), 978-984.
- [26] Ren, D., Fang, J., Liu, P., Sun, X., and Zhang, R. H. (2012). Preparation and property characterization of chitosan/microcrystalline cellulose antimicrobial preservative films. *Applied Mechanics and Materials*, 200, 416-422
- [27] Ren, H., Li, S., Gao, M., Xing, X., Tian, Y., Ling, Z., Yang, W., Pan, L., Fan, W., and Zheng, Y. (2023). Preparation and characterization of microcrystalline cellulose/polylactic acid biocomposite films and its application in lanzhou lily (*Lilium davidii* var. *unicolor*) bulbs preservation. *Sustainability*, 15(18), 13770.
- [28] Suklaw, N., and Ratanakamnuan, U. (2022). Mechanical properties and biodegradability of starch-based biocomposite films reinforced with microcrystalline cellulose from rice embryo. *In Journal of Physics: Conference Series*, 2175(1), 012034.
- [29] Srivastava, K. R., Dixit, S., Pal, D. B., Mishra, P. K., and Srivastava, P. (2021). Environmental technology & innovation effect of nanocellulose on mechanical and barrier properties of PVA – Banana pseudostem fiber composite films. *Environmental Technology & Innovation*, 21, 101312.
- [30] Khalil, R. K., El-sayed, N. B., El-sayed, R. H., Sallam, R. M., Abdelnabi, A. Y., Soliman, N. S., Ibrahim, R. A., Ibrahim, M. A., Sharaby, M. R., and Abdelrahim, D. S. (2025). Guar gum-based systems formulated with encapsulated propolis extract for minimally processed fruits and confectionery packaging. *Food Hydrocolloids*, 169, 111640.
- [31] Yuniarto, K., Lastriyanto, A., and Kurniawan, H. (2020). Permeabilitas oksigen kemasan aktif polylactic acid-butylated hydroxytoluene. *Jurnal Teknologi Pertanian*, 21(2), 136-143.
- [32] Jaime, S. B., Alves, R. M., and Bocoli, P. F. (2022). Moisture and oxygen barrier properties of glass, PET and HDPE bottles for pharmaceutical products. *Journal of Drug Delivery Science and Technology*, 71, 103330.
- [33] Andrés, C. M. C., Pérez de la Lastra, J. M., Juan, C. A., Plou, F. J., and Pérez-Lebeña, E. (2024). Antioxidant metabolism pathways in vitamins, polyphenols, and selenium: Parallels and divergences. *International Journal of Molecular Sciences*, 25(5), 2600.

- [34] Fadlelmoula, A., Pinho, D., Carvalho, V. H., Catarino, S. O., and Minas, G. (2022). Fourier transform infrared (FTIR) spectroscopy to analyse human blood over the last 20 years: A review towards lab-on-a-chip devices. *Micromachines*, 13(2), 187.
- [35] Nandiyanto, A. B. D. (2026). How to read and interpret FTIR spectra for materials: A master dataset with step-by-step guided peak-correlation analysis, representative examples, and a foundation for future artificial intelligence (AI)-assisted analysis. *ASEAN Journal for Science and Engineering in Materials*, 5(2), 323-356.
- [36] Ardyansyah, F., and Yuniwati, M. (2021). Pembuatan plastik biodegradable dari pati umbi ganyong menggunakan plasticizer gliserin dan karagenan (variasi perbandingan massa karagenan dan volume gliserin dengan massa pati). *Jurnal Inovasi Proses*, 6(1), 20-28.
- [37] Nandiyanto, A. B. D., Oktiani, R., and Ragadhita, R. (2019). How to read and interpret FTIR spectroscope of organic material. *Indonesian Journal of Science and Technology*, 4(1), 97-118.
- [38] Iswarin, S. J., Nuriyah, L., and Sriwilujeng, A. I. (2013). Hubungan gugus fungsi plastik biodegradabel metil akrilat dan pati garut terhadap sifat mekaniknya. *Natural B*, 2(2), 178-183.
- [39] Silva, R. R. A., Marques, C. S., Arruda, T. R., Teixeira, S. C., and de Oliveira, T. V. (2023). Biodegradation of polymers: Stages, measurement, standards and prospects. *Macromol*, 3(2), 371-399.
- [40] Nigam, S., Das, A. K., and Patidar, M. K. (2021). Synthesis, characterization and biodegradation of bioplastic films produced from *Parthenium hysterophorus* by incorporating a plasticizer (PEG600). *Environmental Challenges*, 5, 100280.
- [41] Brunšek, R., Kopitar, D., Schwarz, I., and Marasović, P. (2023). Biodegradation properties of cellulose fibers and PLA biopolymer. *Polymers*, 15(17), 3532.
- [42] Chamas, A., Moon, H., Zheng, J., Qiu, Y., Tabassum, T., Jang, J. H., Abu-Omar, M., Scott, S. L., and Suh, S. (2020). Degradation rates of plastics in the environment. *ACS Sustainable Chemistry and Engineering*, 8(9), 3494–3511.
- [43] Zenata, R. (2015). Pembuatan dan karakterisasi kadar air dan gugus fungsi plastik biodegradable berbahan dasar pati umbi walur (*Amorphophallus paenifolius* var. *sylvestris*). *Jurnal Bioproses Komoditas Tropis*, 3(2), 47-52.
- [44] Nnanguma, K. A. (2026). Assessing the impact of soil erosion on rural livelihoods and food security in support of the Sustainable Development Goals (SDGs). *ASEAN Journal of Agriculture and Food Engineering Journal*, 5(1), 1–10.